

## Bulk Dirac Points in Distorted Spinel

Julia A. Steinberg,<sup>1,2,\*</sup> Steve M. Young,<sup>1</sup> Saad Zaheer,<sup>2</sup> C. L. Kane,<sup>2</sup> E. J. Mele,<sup>2</sup> and Andrew M. Rappe<sup>1</sup>

<sup>1</sup>*The Makineni Theoretical Laboratories, Department of Chemistry, University of Pennsylvania, Philadelphia, Pennsylvania 19104-6323, USA*

<sup>2</sup>*Department of Physics and Astronomy, University of Pennsylvania, Philadelphia, Pennsylvania 19104-6396, USA*

(Received 23 September 2013; published 22 January 2014)

We report on a Dirac-like Fermi surface in three-dimensional bulk materials in a distorted spinel structure on the basis of density functional theory as well as tight-binding theory. The four examples we provide in this Letter are BiZnSiO<sub>4</sub>, BiCaSiO<sub>4</sub>, BiAlInO<sub>4</sub>, and BiMgSiO<sub>4</sub>. A necessary characteristic of these structures is that they contain a Bi lattice which forms a hierarchy of chainlike substructures, with consequences for both fundamental understanding and materials design.

DOI: 10.1103/PhysRevLett.112.036403

PACS numbers: 71.18.+y, 71.27.+a, 81.05.Zx

Following the discovery of topological insulators [1], there has been considerable interest in studying semimetallic phases that exist at the phase transition between a topological and a trivial insulator. One such example is graphene, which has two Dirac points at its Fermi surface. A Dirac point is characterized by four degenerate states that disperse linearly with momentum around a single point  $\mathbf{k}$  in the Brillouin zone. The resulting low energy theory is pseudorelativistic, and it is responsible for many of the interesting properties of graphene [2]. In a previous communication, we described such Dirac points occurring as symmetry-protected fourfold degeneracies in three-dimensional crystal systems. Such a Dirac point was encountered first in a tight-binding model of  $s$  states on the diamond lattice [3]. We showed that the occurrence of this Dirac point is a feature of the symmetry of diamond, which occurs in space group 227. While no realistic system of atoms in a primitive diamond lattice produces this feature, through first-principles calculations we found that substituting bismuth for silicon in  $\beta$ -cristobalite, also in space group 227, elevates a candidate Dirac point degeneracy to the Fermi level, making BiO<sub>2</sub> the first realistic Dirac semimetal proposed [4]. While this material is predicted to be metastable, it is highly unfavorable thermodynamically. This led us to consider alternative crystal structures and symmetries. Three-dimensional Dirac points have also been predicted to exist at the phase transition between a topological and a normal insulator when inversion symmetry is present [5,6]. If either inversion or time-reversal symmetry is broken at the transition, a Dirac point separates into Weyl points which have been shown to exist in Refs. [7–9]. Here we find, on the basis of density functional theory and tight-binding calculations, that a family of three-dimensional materials in a distorted spinel structure supports robust Dirac points in their bulk electronic spectra. A common characteristic of these materials is the presence of a hierarchy of chainlike substructures created by the bismuth atoms in the  $A$  site of the crystal structure.

The spinel structure hosts a family of chalcogenides which have the general formula  $AB_2X_4$ .  $A$  and  $B$  are cations that are coordinated by anions of species  $X$ , which may be O, S, Se, or Te. The  $A$  sites are tetrahedrally coordinated in a diamond lattice, with the octahedrally coordinated  $B$  sites in the interstices [10]. Most known spinels are insulators with band gaps of a few eV; this natural tendency toward insulating behavior makes the spinel structure a prime candidate to host a material with a distinct Dirac point degeneracy formed by bands that do not elsewhere cross the Fermi level. By contrast, though the Laves structure contains the required symmetry for a Dirac point, materials in this structure tend to be metallic and our attempts to engineer Dirac semimetals in this structure were plagued by additional band crossings at the Fermi level.

BiAl<sub>2</sub>O<sub>4</sub> and BiSc<sub>2</sub>O<sub>4</sub> in the spinel structure exhibit Dirac points at the  $X$  points in the Brillouin zone (BZ). However, these materials are not stable and spontaneously break symmetry. Fortunately, one of the child symmetry groups is space group 74, which our crystallographic symmetry criteria [4] admit as a potential host for a Dirac semimetal. As shown in Fig. 1, the cubic unit cell distorts to an orthorhombic cell and the bismuth atoms shift from their previous locations along one of the axes of twofold rotation symmetry in the diamond lattice. This symmetry breaking also distinguishes the two  $B$  atoms of the formula unit, which we label  $B'$  and  $B''$  Figs. 1 and 2, so that the composition becomes Bi $B'B''$ O<sub>4</sub>. While this new space group has much lower symmetry, it inherits the nonsymmorphic symmetry of diamond and retains one of the three Dirac points among its representations. This Dirac point occurs at the point  $T$  in the BZ and, as in diamond, there is a gap at  $W$  determined by the strength of the spin-orbit interaction. The effects of reduced symmetry are manifest in the elongation of the octahedral cages of the  $B'$  site. This allows the diamond lattice of bismuth to separate into distinct, parallel zig-zag chains. Through first principles DFT calculations we have determined that BiZnSiO<sub>4</sub>, BiCaSiO<sub>4</sub>,

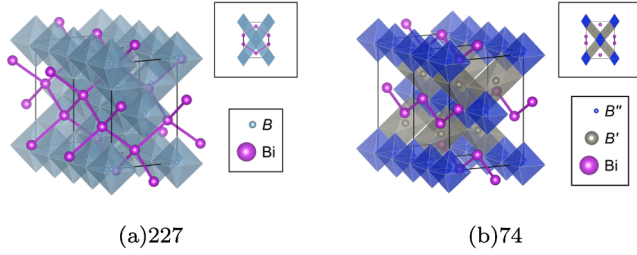


FIG. 1 (color online). The (a) spinel and (b) distorted spinel structures. Conventionally, the high-symmetry spinel unit cell is cubic; here we have chosen a reduced supercell allowing for direct comparison with the distorted structure. The  $A$  sites, populated by Bi, are surrounded by a tetrahedral oxygen cage (not shown for clarity) and the  $B$  sites are surrounded by octahedral oxygen cages. In the high-symmetry spinel all Bi neighbors are equidistant, and the Bi atoms form a diamond lattice. Upon distortion, bonds lying in the  $(0, 1, 0)$  plane elongate, and the structure can be described as coupled, close-packed, corrugated chains running parallel to  $[0, 1, 0]$ .

$\text{BiAlInO}_4$ , and  $\text{BiMgSiO}_4$  are each metastable and exhibit Dirac point degeneracies at  $T$  with no other band crossings at the Fermi level (Fig. 3). Both the crystal and electronic structures are very similar for these materials, and in the following we take  $\text{BiZnSiO}_4$  to be representative of all four. For these electronic structure and atomic relaxation calculations, we used the plane wave density functional theory package QUANTUM ESPRESSO [11] and designed non-local pseudopotentials [12,13] with spin-orbit interaction generated by OPIUM. For all calculations an energy cutoff of 50 Ry and  $k$ -point grids of  $8 \times 8 \times 8$  for the primitive cell were used.

The states near the Fermi surface are dominated by  $p$ -like states on the Bi atoms, as revealed by the angular-momentum-projected density of states in Fig. 4(a), suggesting that each Bi possesses a pair of  $5s$  electrons and an unpaired  $5p$  electron. This contrasts with both the Fu-Kane-Mele tight-binding model and  $\text{BiO}_2$ , where the electronic character of the Dirac point derives from an unpaired  $5s$  electron. The presence of an unpaired electron is required by symmetry considerations. Nonsymmorphic space groups have at least one sublattice degree of freedom, and at the  $\mathbf{k}$  points hosting Dirac points, the only representations are fourfold. Thus, for a fourfold degeneracy to be bisected by the Fermi level there must be an odd number of electrons per formula unit. This symmetry constraint signifies physics being driven by these unpaired electrons. In Fig. 4(c) the Bloch states (excluding the spin degree of freedom) of the Dirac point degeneracy are shown, with a cartoon representation in Fig. 4(b) added for clarity. The character of these states confirms that the unpaired  $p$  electrons give rise to the observed Dirac point physics: the two states are related by the symmetry between the two bismuth sublattices that makes the space group nonsymmorphic. Additionally, the system must lie at a critical point between

the two configurations where bismuth atoms pair into dimers and is protected by the sublattice symmetry in all three directions; otherwise the interaction between the zig-zag chains could gap the system. This symmetry, which prevents the unpaired electrons from forming bonds in either direction, only belongs to the little group at  $T$ ; elsewhere it is absent and the degeneracy between the two states is lifted. These chains are reminiscent of polyacetylene, which is characterized by a pattern of alternating single and double bonds along carbon sites leading to a twofold degenerate ground state. This suggests that the individual chains of bismuth sites behave like coupled one-dimensional metal wires running through an otherwise insulating structure. An isolated chain of this kind would be described by the Su-Schrieffer-Heeger [14] model and would suffer from the Peierls instability intrinsic to the half-filled state, breaking the Dirac point. However, the coupling between the chains (Fig. 2) requires a three-dimensional model, and the stability against dimerization depends on microscopic details. First, upon dimerization, the oxidation state of bismuth becomes defined as  $2+$ . This is highly unfavorable for bismuth, which is known to prefer oxidation states of  $3+$  or  $5+$ . Second, the other cations are small, encouraging a more closely packed lattice and increasing the favorability of the delocalized, metallic character of the Dirac point. Thus the critical point, where the oxidation state of bismuth is formally undefined and the unpaired electrons are delocalized, is locally stable.

Focusing now on the bismuth lattice, Fig. 2 shows an annotated structure of a distorted spinel. The bismuth atoms form a chainlike structure going into the plane, and adjacent chains have a different ordering of the two types of bismuth atoms. Figure 2(a) illustrates chains of  $\alpha$ - and  $\beta$ -type Bi atoms along the  $y$  axis, while Fig. 2(b) illustrates that adjacent atoms along the  $x$  and  $z$  axes form an additional chainlike structure. Therefore the Dirac point at  $T$  can be understood to be arising from three levels of chainlike structures, resulting in a Dirac point that is protected by the sublattice symmetry of space group 74.

We may model the low-energy theory of distorted spinels by a tight-binding model of  $p$  states on the Bi atoms. The two bismuth atoms in each unit cell each have  $p_x$ ,  $p_y$ , and  $p_z$  orbitals. We distinguish between the two bismuth sites (and associated sublattices) with the labels  $A$  and  $B$ . There are four bonds possible for each site; these are  $\mathbf{d}^{1\pm} = (\pm a/2, 0, [1 - 2\gamma]c)$  and  $\mathbf{d}^{2\pm} = (0, \pm b/2, 2\gamma c)$ , where  $a$ ,  $b$ , and  $c$  are the lengths of the orthorhombic lattice vectors, and  $\gamma$  describes an internal distortion; when  $a = b = c/\sqrt{2}$  and  $\gamma = 1/8$ , the lattice becomes diamond. Excluding spin for the moment, the tight-binding Hamiltonian becomes

$$\mathcal{H}_{\text{tb}} = \sum_{\langle ij \rangle} c_{i,\alpha}^\dagger c_{j,\beta} [(t_\sigma - t_\pi)(\alpha \cdot \mathbf{d}_{ij})(\beta \cdot \mathbf{d}_{ij}) + t_\pi(\alpha \cdot \beta)]. \quad (1)$$

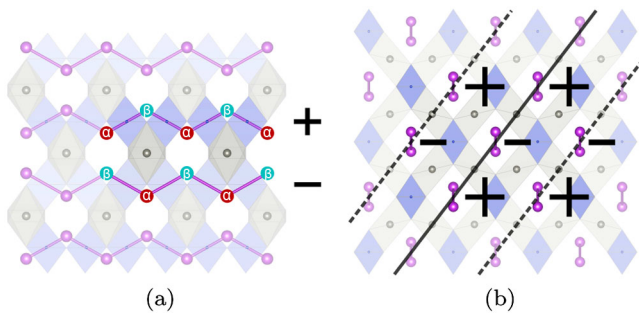


FIG. 2 (color online). The distorted spinel structure with the Bi network annotated.  $B''$  cages are blue,  $B'$  cages are gray, and the Bi atoms are in purple. The chains (a) are composed of Bi atoms with alternating bond directions, labeled  $\alpha$  and  $\beta$ , forming chains with distinct orientations from their nearest neighbors, signified by + and -. Running parallel to  $[0, 1, 0]$ , the alternately oriented chains form their own chainlike structure in the  $[1, 0, 1]$  direction, so that each chain is now an object coupling to its neighbors in 1D. The resulting parallel planes of alternating sense (denoted by solid and dashed lines), constructed from the sheets of coupled chains, themselves couple with one another in the  $[1, 0, -1]$  direction. Thus, at each level of structure the elements (atoms, chains, and planes) alternate in orientation along a particular direction, resulting in a fourfold representation for a point on the BZ surface corresponding to one half of a reciprocal lattice vector for each of those directions, and a Dirac point at the Fermi level for half-filling.

The bismuth sites are indexed by  $i$  and  $j$ , and the sets of  $p$ -orbital orientations for site  $i$  are labeled by  $\alpha$  whereas those for site  $j$  are labeled by  $\beta$ , which may be the unit vectors  $\hat{x}$ ,  $\hat{y}$ , and  $\hat{z}$ .  $t_\sigma$  and  $t_\pi$  are phenomenological coupling parameters for the  $\sigma$  and  $\pi$  character of the  $p$ - $p$  bonds, and  $\mathbf{d}_{ij}$  is one of the aforementioned bond vectors that connect sites  $i$  and  $j$ .

The resulting Hamiltonian produces three pairs of bands, each with a degeneracy from  $T$  to  $W$ , with bonding and antibonding pairs split off below and above the middle non-bonding pair by energy proportionate to  $|t_\sigma - t_\pi|$ . Since each bismuth contributes a single electron, we expect the lowest, bonding pair of bands to be half-filled. By inspection we find that these bands at  $T$  are dominated by the  $p$  orbitals in the plane of the chain, corroborating our first principles results, and confirming that the crucial physics is due to the bismuth lattice. Introducing a spin-orbit term of the form

$$\mathcal{H}_{\text{so}} = \sum_{\langle\langle ij \rangle\rangle, s, s', \alpha, \beta} i\lambda_{i\alpha j\beta} \mathbf{d}_{ij}^1 \times \mathbf{d}_{ij}^2 \cdot \vec{\sigma}_{ss'} c_{i, \alpha s}^\dagger c_{j, \beta s'}, \quad (2)$$

where  $\mathbf{d}_{ij}^1$  and  $\mathbf{d}_{ij}^2$  are nearest neighbor bond vectors that connect sites  $i$  and  $j$  on the same sublattice, we find that the degeneracies at  $W$  are split, allowing Dirac points at  $T$ . The effect, however, is not strong enough to mix the three sets of bands with one another, again in agreement with first-principles calculations. Removing the distortion

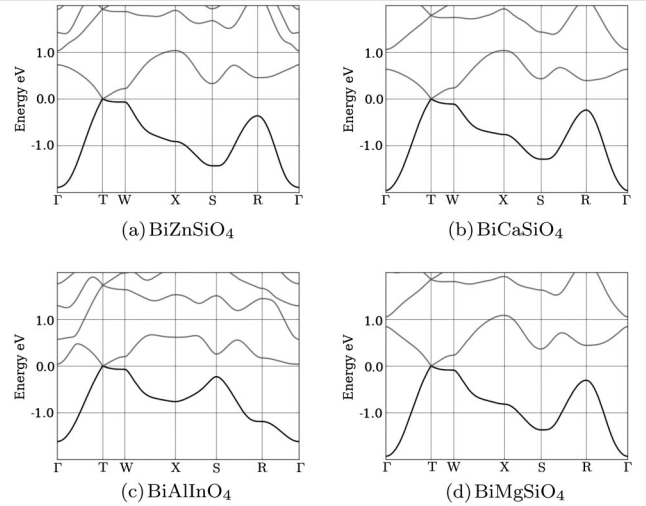


FIG. 3. The band structures of  $\text{BiZnSiO}_4$  (a),  $\text{BiCaSiO}_4$  (b),  $\text{BiAlInO}_4$  (c), and  $\text{BiMgSiO}_4$  (d) in the distorted spinel structure all contain a Dirac point at  $T$  that is completely split along the line in the Brillouin zone from  $T$  to  $W$  due to the spin orbit interaction between the bismuth sites in the lattice.

in space group 74 to restore the diamond lattice in Eq. (2) provides the three Dirac points originally known to exist at the  $X$  points in diamond. Thus, high symmetry diamond exists as a critical point between the single Dirac-point phases allowed by the three directions in which the symmetry may be reduced to space group 74. This provides a simple understanding of how the Dirac point in diamond is connected to the Dirac point in space group 74.

To evaluate the possibility of synthesizing a Dirac semimetal in the laboratory, we calculated the energy difference associated with synthesizing  $\text{ZnBiSiO}_4$  from zinc silicate, bismuth metal, and oxygen gas, and found that the  $\text{ZnBiSiO}_4$  distorted spinel structure is lower in energy by about 0.25 eV per formula unit. A major challenge involved in this synthesis would be to prevent bismuth from further oxidizing and causing the constituents to segregate. The conventionally determined oxidation state of bismuth appears to pose a significant obstacle in synthesizing the proposed materials. However, that this oxidation state characterizes nearby insulating states is crucial to providing an odd electron formula unit and stabilizing the Dirac-semimetal state. Similar configurations of bismuth atoms have been achieved in the laboratory in the construction of bulk materials built from stacks of two-dimensional topological insulators [15]. We therefore propose that synthesis be conducted under reducing conditions (high temperature and low partial pressure of  $\text{O}_2$ ).

Finally, we note that additional symmetry breaking may allow access to exotic insulating phases. The low-energy theory at the Fermi surface can be written as  $\mathcal{H}(\mathbf{k}) = v_x k_x \gamma_x + v_y k_y \gamma_y + v_z k_z \gamma_z$ , centered at  $T$ , where  $v_i$  are the Fermi velocities and  $\gamma_i$  are  $4 \times 4$  Dirac matrices.

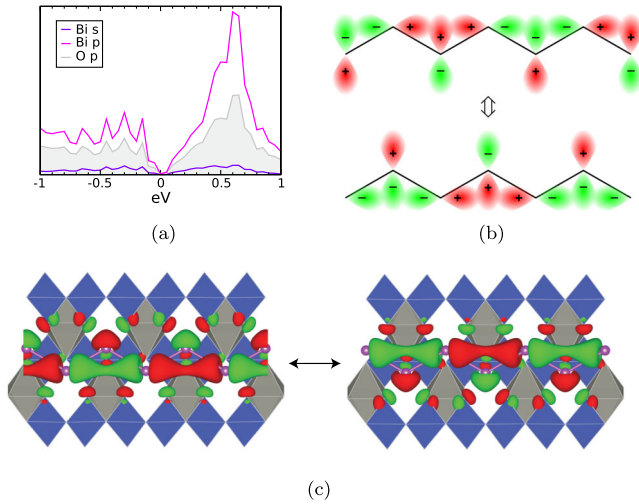


FIG. 4 (color online). Projected density of states near the Dirac point in the  $\text{ZnBiSiO}_4$  structure (a). States near the Dirac point are primarily Bi  $p$  states, with a vanishing density at the Fermi energy. The angular portion of the wave functions (i.e., without the spin degree of freedom) of the  $\text{ZnBiSiO}_4$  structure at  $T$  is shown in (c), with a cartoon depiction in (b) emphasizing their  $p$ -like nature. The neighboring bismuth sites interact in a way that can be depicted as chains of Bi  $p$  orbitals running through an insulating structure, in which individual chains are analogous to polyacetylene; nonsymmorphic operation of “inversion followed by translation between  $A$  sites” results in an equivalent but different state, creating a twofold degeneracy at the Dirac point, which then becomes fourfold due to the spin degree of freedom. Breaking inversion symmetry in this structure is analogous to having inequivalent coupling constants between Bi sites and single and double bonds in polyacetylene, and will lift the degeneracy, gapping the system.

The Dirac matrices are constrained by the invariance of  $\mathcal{H}(\mathbf{k})$  under the little group at  $T$ . Orienting the  $k_z$  axis to point along the line from  $T$  to  $\Gamma$ ,  $\mathcal{H}(\mathbf{k})$  takes the form,

$$\mathcal{H}(\mathbf{k}) = v_x k_x \sigma_x \otimes \sigma_z + v_y k_y (\cos \theta \sigma_x \otimes \sigma_x + \sin \theta \sigma_x \otimes \sigma_y) + v_z k_z \sigma_y \otimes \mathbb{1}. \quad (3)$$

Here  $\theta$  is an arbitrary real parameter,  $\sigma_i$  are the usual Pauli matrices, and  $\mathbb{1}$  is the  $2 \times 2$  identity matrix. The exact values of  $\theta$  and  $v_i$  depend on microscopic features.

The elements of the little group that stabilize the Dirac point at  $T$  are: mirror symmetry  $\mathcal{M}_z$  about the  $k_x k_y$  plane, sublattice (inversion) symmetry  $\mathcal{I}$ , and time-reversal symmetry  $\Theta$ . In the basis of Eq. (3), these operators can be represented as,  $\mathcal{M}_z = \sigma_x \otimes \mathbb{1}$ ,  $\mathcal{I} = \sigma_z \otimes \mathbb{1}$ , and  $\Theta = i\sigma_y \otimes \mathbb{1} K$  where  $K$  denotes complex conjugation. Symmetry breaking perturbations lead to insulating (topological and normal) as well as topological semimetallic (Weyl) phases. The distorted spinel structures discussed in this Letter, if engineered or discovered naturally, can be used to access such phases. Dirac semimetals are unique in that they

exist at a multicritical point from which many exotic insulating and topological semimetallic phases can be reached [4].

We emphasize that the crucial feature of these materials is the network of interpenetrating, symmetry-related sublattices of bismuth atoms with unpaired electrons, a physical manifestation of the symmetry-derived result that Dirac points can only exist in nonsymmorphic space groups on the BZ surface. The rest of the atoms of the lattice can be thought of as an insulating scaffolding that stabilizes this metallic bismuth network that hosts the Dirac point. The combination of close packing and unconventional oxidation state reduces the tendency towards dimerization and the system remains at the critical point of this half-filled state. These offer important insight into both the physics and materials science of the Dirac semimetal state, and will inform efforts to realize such a material.

This work was supported in part by the MRSEC program of the National Science Foundation under Grant No. DMR11-20901 (S. M. Y.), by the Department of Energy under Grant No. FG02-ER45118 (E. J. M. and S. Z.), and by the National Science Foundation under Grants No. DMR11-24696 (A. M. R.) and No. DMR09-06175 (C. L. K.). J. A. S. was supported by the REU program at LRSM, University of Pennsylvania, and by the Department of Energy under Grant No. DE-FG02-07ER46431. S. M. Y. acknowledges computational support from the High Performance Computing Modernization Office.

*Note added.*—We have recently learned of two independent experiments [16,17] that report the existence of a three-dimensional Dirac point in  $\text{Cd}_3\text{As}_2$ . We note that the mechanism underpinning the Dirac point in this material combines band inversion with rotational symmetry [18], which is different from our theory that relies solely on crystal symmetry. However, these experiments show that the Dirac semimetal phase is stable, despite the Fermi level being somewhat above the Dirac point due to disorder, and that the Dirac point is responsible for the high electron mobility in  $\text{Cd}_3\text{As}_2$ . We hope that these insights will accelerate efforts to observe similar Dirac points in distorted spinels.

\*Corresponding author.  
stjulia@sas.upenn.edu

- [1] C. L. Kane and E. J. Mele, *Phys. Rev. Lett.* **95**, 226801 (2005).
- [2] A. H. C. Neto, F. Guinea, N. M. R. Peres, K. S. Novoselov, and A. K. Geim, *Rev. Mod. Phys.* **81**, 109 (2009).
- [3] L. Fu, C. L. Kane, and E. J. Mele, *Phys. Rev. Lett.* **98**, 106803 (2007).
- [4] S. M. Young, S. Zaheer, J. C. Y. Teo, C. L. Kane, E. J. Mele, and A. M. Rappe, *Phys. Rev. Lett.* **108**, 140405 (2012).
- [5] S. Murakami, *New J. Phys.* **9**, 356 (2007).

- [6] S. M. Young, S. Chowdhury, E. J. Walter, E. J. Mele, C. L. Kane, and A. M. Rappe, *Phys. Rev. B* **84**, 085106 (2011).
- [7] X. Wan, A. M. Turner, A. Vishwanath, and S. Y. Savrasov, *Phys. Rev. B* **83**, 205101 (2011).
- [8] A. A. Burkov and L. Balents, *Phys. Rev. Lett.* **107**, 127205 (2011).
- [9] G. B. Halász and L. Balents, *Phys. Rev. B* **85**, 035103 (2012).
- [10] J. K. Burdett, G. D. Price, and S. L. Price, *J. Am. Chem. Soc.* **104**, 92 (1982).
- [11] P. Giannozzi *et al.*, *J. Phys. Condens. Matter* **21**, 395502 (2009).
- [12] A. M. Rappe, K. M. Rabe, E. Kaxiras, and J. D. Joannopoulos, *Phys. Rev. B* **41**, 1227 (1990).
- [13] N. J. Ramer and A. M. Rappe, *Phys. Rev. B* **59**, 12471 (1999).
- [14] W. P. Su, J. R. Schrieffer, and A. J. Heeger, *Phys. Rev. Lett.* **42**, 1698 (1979).
- [15] B. Rasche, A. Isaeva, M. Ruck, S. Borisenko, V. Zabolotnyy, B. Büchner, K. Koepf, C. Ortix, M. Richter, and J. van den Brink, *Nat. Mater.* **12**, 422 (2013).
- [16] S. Borisenko *et al.*, arXiv:1309.7978.
- [17] M. Neupane *et al.*, arXiv:1309.7982.
- [18] Z. Wang, H. Weng, Q. Wu, X. Dai, and Z. Fang, *Phys. Rev. B* **88**, 125427 (2013).